AeroBest 2021

International Conference on Multidisciplinary Design Optimization of Aerospace Systems

Proceedings

21–23 July 2021
Lisboa, Portugal

André C. Marta & Afzal Suleman (editors)

Published by:
IDMEC
Instituto Superior Técnico
Universidade de Lisboa
Portugal
https://aerobest2021.idmec.tecnico.ulisboa.pt/

ISBN: 978-989-99424-8-6

Editors:
André C. Marta
Afzal Suleman

AeroBest 2021
Lisboa, 21-23 July 2021

THE CONCEPT OF SELF-DEPLOYABLE HELIUM-FILLED AEROSTATS BASED ON TENSEGRITY STRUCTURES

Lech Knap[1], Andrzej Świercz[2], Cezary Graczykowski[2*], Jan Holnicki-Szulc[2]

1: Institute of Vehicles and Construction Machinery
Warsaw University of Technology
Narbutta 84, 02-524 Warsaw, Poland
Lech.Knap@pw.edu.edu, http://www.simr.pw.edu.pl

2: Institute of Fundamental Technological Research
Polish Academy of Sciences
Pawinskiego 5B, 02-106 Warsaw, Poland
{aswiercz, cgraczyk, holnicki}@ippt.pan.pl, http://www.ippt.pan.pl

Abstract *In this contribution, the authors propose a concept of novel type of an ultra-light helium-filled aerostat. The internal construction of the proposed aerostat is based on a self-deployable tensegrity structure equipped with prestressed tensioned elements of controllable lengths. Such construction enables convenient transportation of the aerostat and its fast deployment at the required operational point at the atmosphere. The controllable tensegrity structure can be used for simultaneous changes of the aerostat volume and external shape during the flight. This enables modification of buoyancy and drag forces and obtaining a desired vertical and horizontal motion as well as a desired flight path. The authors propose a method of numerical modelling of self-deployable helium-filled aerostats based on the finite element method as well as CFD and FSI models presenting behaviour of aerostat during typical operational conditions. The presented results show the interaction of the internal tensegrity structure and aerostat envelope and positively verify the feasibility of the proposed concept of tensegrity-based aerostats.*

Keywords: tensegrity structure, internal construction, helium-filled aerostat, numerical modelling

1. INTRODUCTION

Airships and balloons were the first vehicles built by men but for many years their applications have been very limited due to intensive development of aviation. Specified military application of airships included reconnaissance missions, combat of submarines and ocean surveillance [1-2], while the attempts of their civil use were interrupted for many years by well-known crash of the Hindenburg airship in 1937 [3]. However, recent technological changes have caused renaissance of airship applications. At the beginning of the century many new-generation helium-filled airships with the ability to undertake long-term and low-energy flights have been constructed and initially used for low-cost missions aimed at exploration of stratosphere and mesosphere [4-6]. Currently constructed airships provide telecommunication systems in rarely populated areas, serve as remote monitoring or surveillance systems and research pseudo-satellites [7-10]. The most well-known examples of airships are Zephyr S [11], Russian concept Berkut [12], Lockheed Martin's ISIS [13] and French Stratobus [14].

Significant effort in the design of airships is focused on the reduction of the self-weight, which largely influences the load capacity and the possibility of carrying payloads. The first technological challenge in construction of airships is development of ultra-light envelopes of thickness of several micrometers, which are helium-tight and maintain elastic properties at wide range of temperatures [15]. The second important technological problem is design of skeletal structure which supports airship envelope and provides its appropriate shape and resistance to aerodynamic forces. The related challenge is designing connections of the internal skeletal structure and airship envelope and attachment of the cargo to this fragile structure.

In this paper the authors propose construction of the aerostat based on deployable tensegrity structure equipped with elements of controllable lengths. Such construction enables convenient transport of the aerostat with the use of a balloon or an aircraft to the operational altitude and its automatic deployment at certain location at the atmosphere. The tensegrity structure provides very low mass of the aerostat, adequate strength to support the aerostat envelope during strong wind gusts and possibility of transferring point loads resulting from carried cargo. On the other hand, application of tensegrity structure equipped with controllable elements enables convenient change of the aerostat volume and shape during the flight. The change of volume is used to control the actual buoyancy force and resulting vertical motion of the aerostat ("V-mobility"). In turn, the change of aerostat shape can be used for changing the influence of lateral wind gusts or controlling horizontal stability or positioning during the mission ("H-stability").

The paper is organized as follows. The second section describes general construction of aerostats based on the tensegrity structures and details of the proposed design. The third section shows FEM-based strength analysis of the aerostat including distributions of internal forces caused by pressure differences. The fourth section presents CFD analysis of the flow around aerostat and simplified FSI analysis revealing an interaction of the flow and the tensegrity-supported aerostat envelope. Finally, the fifth section concludes the conducted research.

2. CONSTRUCTION OF TENSEGRITY-BASED AEROSTATS

The simplest proposed tensegrity-based aerostat utilizes skeletal structure in the form of tensegrity prism which is composed of three struts and nine tendons (Fig.1a). While the selected nodes (1a) of the tensegrity structure are permanently integrated with the aerostat envelope, the

other nodes (1b) are linked in slidable fashion to avoid excessive internal forces in both substructures. In considered case three vertical tendons (denoted as (1e), green-coloured) are highly elastic, while the length of three horizontal stiff tendons (denoted as (1e), blue-coloured) can be controlled. The proposed structure is distinguished from the classic tensegrity structure by highly elastic tendons (1e) with a much lower Young's modulus than Young's modulus for the other elements. A structural stability of the structure is ensured by the red-coloured bars (1d). The aerostat based on such a tensegrity structure can be cylindrical-shaped with two hemispheres located at the lateral sides (Fig.1b). Symmetric shortening of the stiff tendons of controllable lengths implies change of the radius along the cylinder, decease of volume of the aerostat and causes that its shape becomes slender. In turn, asymmetric shortening of the tendons causes asymmetric deformation of the aerostat and changes it resistance to winds in axial direction.

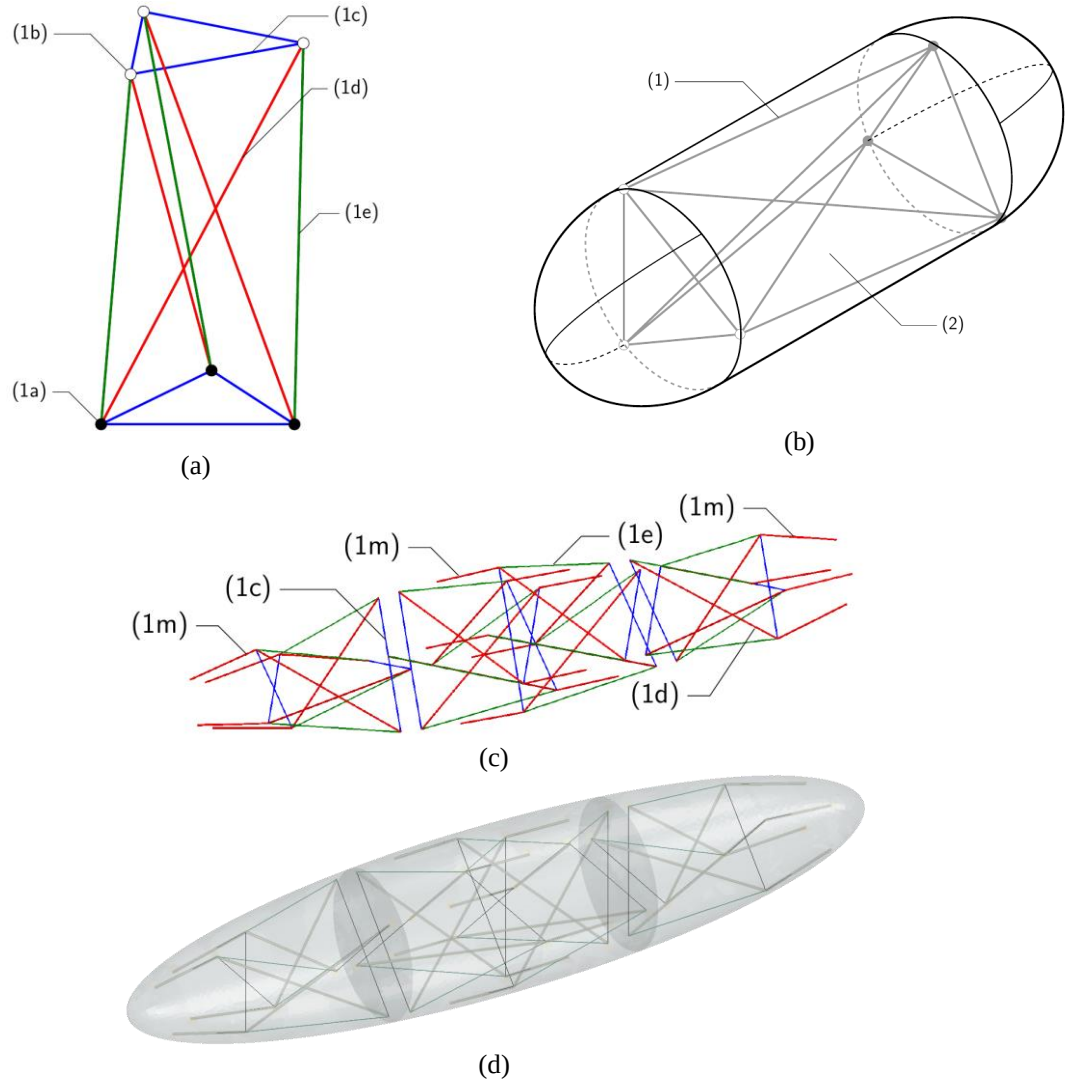

Figure 1. (a) A single module of foldable tensegrity structure; (b) a single-chambered tensegrity-based aerostat; (c) a four-module tensegrity structure; (d) a tree-chamber aerostat with four modules of tensegrity structure.

The more complex tensegrity-based ellipsoid-shaped aerostat, considered in further part of this paper is composed of four modules of tensegrity structure. Each unit is based on two squares rotated by 45 degrees (Fig.1c-d). Contrary to the previous case, stiff tendons (1c) are arranged into crosses instead of peripherally. The struts, highly elastic and controllable tendons are shown in Fig.1c. Additionally, the set of movable joints of each unit tensegrity structure is slidingly connected to guide rails (1m) which are bounded to the aerostat envelope.

In this case the shape of the aerostat is based on ellipsoid with a circular cross-section in the vertical plane. The considered aerostat is 10 metres long and 2 m wide and it is divided into three chambers with the use of two internal diaphragms. Similarly, as in the case of single-chambered aerostat, the shortening of the tendons causes decrease of aerostat radius and reduction of its volume. Nevertheless, the application of four modules of the tensegrity structure provides wide possibilities of change of the aerostat shape (two modules are placed in the middle chamber). In the proposed solution, shape of the arbitrary section of the aerostat can be significantly modified, which causes that aerostat can be precisely adjusted to wind gusts in both axial and lateral directions (the process of "adaptive morphing").

The above process of changing the length of tendons can be efficiently conducted using controllable retractors, such as rotary electric motors or linear actuators, serving for contraction or elongation of stiff tendons (1c). Let us note that shortening of tendons of tensegrity structure leads to substantial redistribution of internal forces in the entire tensegrity structure and affects deformations and stresses generated in the aerostat envelope.

3. STRENGTH ANALYSIS OF TENSEGRITY-BASED AEROSTAT

This section presents the results of FEM-based strength analysis aimed at finding distributions of internal forces in skeletal structure and envelope of the aerostat caused by pressure differences at various altitudes. A numerical model of the aerostat presented in Fig.1d was created using Abaqus package. The mesh of the envelope and nodes of the tensegrity structure are illustrated in Fig.2.

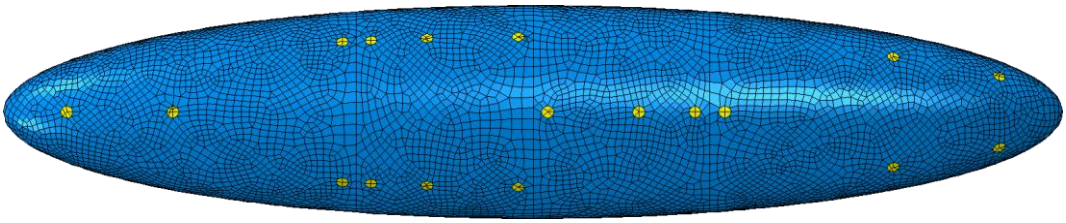

Figure 2. A numerical model of a three-chamber aerostat with four internal modules of tensegrity structure.

The envelope and diaphragms are modelled by means of 3-node and 4-node membrane finite elements. However, in the locations of connection with non-movable tensegrity joints and guide rails, the stiffening plates (yellow-coloured in Fig.2) are applied and modelled by shell finite elements. The internal structure is modelled by truss elements (highly elastic tendons), beam elements (bars and guide rails) and connectors (stiff tendons, retractors and sliding connections). The connector element-type is applied to define interaction between two points and it is useful for control of tendon lengths by means of retractors. The total number of finite

elements in the model is equal to 13 811. For computations, the following material data was assumed:

- envelope and diaphragms: thickness 50 μm, density 1390 kg/m^3 and Young's modulus 0.43 GPa;
- bars, guide rails (both pipe cross-section, diameter of 12 mm and thickness of 1 mm) and stiffening plates (thickness of 1 mm) are made of carbon fibre with density of 1580 kg/m^3 and Young modulus of 87.0 GPa;
- highly elastic tendons (rubber-like material): circular cross-section with diameter of 3.6mm, density of 900 kg/m^3 and Young modulus of 0.05 GPa;
- stiff tendons: circular cross-section with diameter of 3 mm, density of 7850 kg/m^3 and Young's modulus of 210 GPa.

The total mass of the aerostat (including payload) is equal to 15.172 kg. A structural strength assessment of the aerostat was performed for three altitudes: h_2=5 km, h_1=3.725 km and h_s=2 km. Firstly, to reach the altitude of h_2, helium mass of 2.537 kg was inflated into the aerostat. Then, aerostat was partially deflated and helium was compressed in an additional tank (of 0.095 kg to lower the altitude). Finally, all stiff tendons were uniformly shortened to achieve the altitude of h_s=2 km. Outer atmospheric pressure in the numerical model is applied outwardly to the aerostat envelope and linearly varies from ground level to the target altitude. The quasi-static calculations were based on NASA's atmosphere model available on the web site https://www.grc.nasa.gov/www/K-12/airplane/atmosmet.html.

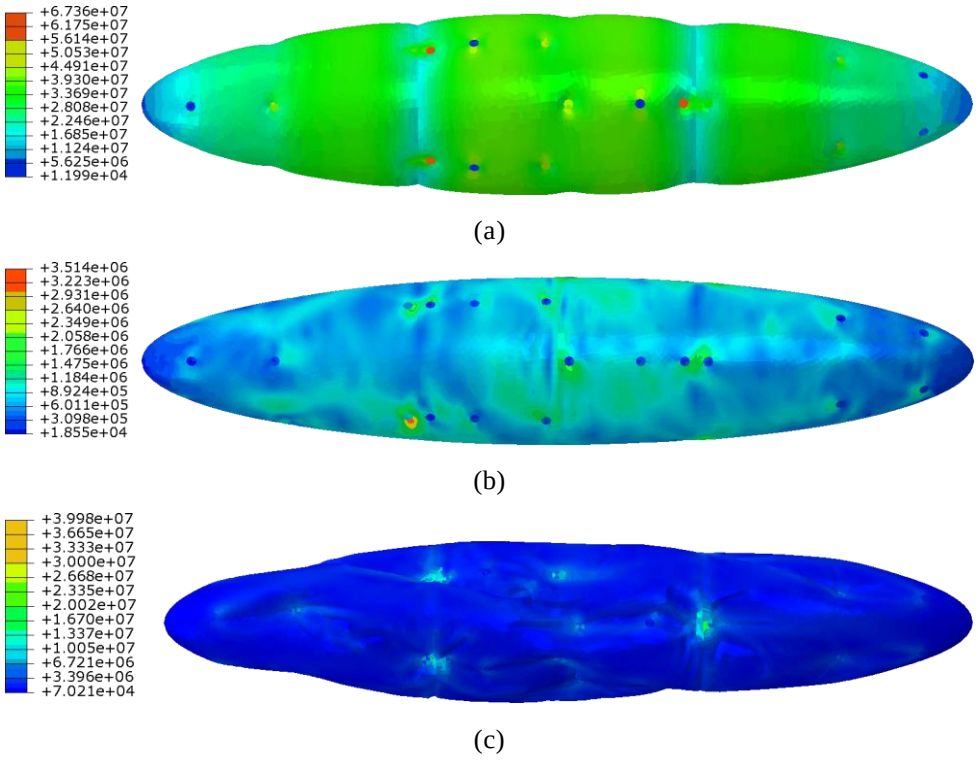

Figure 3. The equivalent von Misses stresses in the envelope at altitude of (a) h_2=5 km, (b) h_1=3.725 km and (c) h_s=2 km.

The obtained results are presented in Fig.3 and Fig.4. In Fig.3 equivalent Mises stresses in the envelope computed for the aforementioned altitudes are presented. The highest level of the equivalent Mises stresses is reached for the altitude of h_2=5 km – about 50MPa in the membrane and 67MPa in the stiffening plates. While the aerostat descents to the altitude h_1=3.725 km (as a results of partial helium compressing), the equivalent Mises stresses are also decreasing. When the aerostat continues its descent by shortening tendons, the stresses level in the bar members sharply increases to 240 MPa , as illustrated in Fig.4 (longitudinal stresses), but they do not exceed the yield stresses limit.

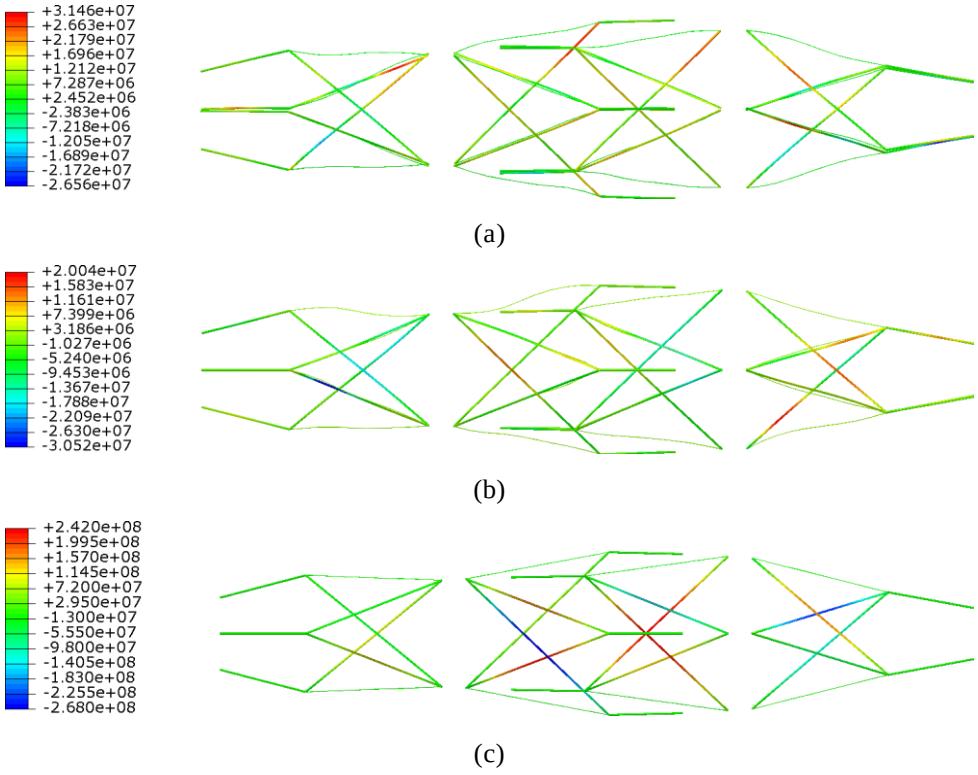

Figure 4. Longitudinal stresses in tensegrity structure elements at altitude of (a) h_2=5 km, (b) h_1=3.725 km, (c) h_s=2 km.

4. CFD AND FSI ANALYSIS OF TENSEGRITY-BASED AEROSTAT

The section presents CFD analysis of the flow around aerostat in vertical and horizontal direction as well as simplified FSI analysis revealing interaction of the vertical flow and envelope of the aerostat supported by the tensegrity structure.

4.1. CFD analysis

The simulations of the flow around the aerostat were aimed at determination of the flow profiles, computation of pressures exerted at certain points of aerostat envelope and calculation of total forces exerted on the aerostat. The analysis was conducted using ANSYS Fluent and was performed for both lateral and axial direction of the flow (Fig.5a-b and Fig.5c-d, respectively). The results of the conducted analyses were used to determine change of the drag

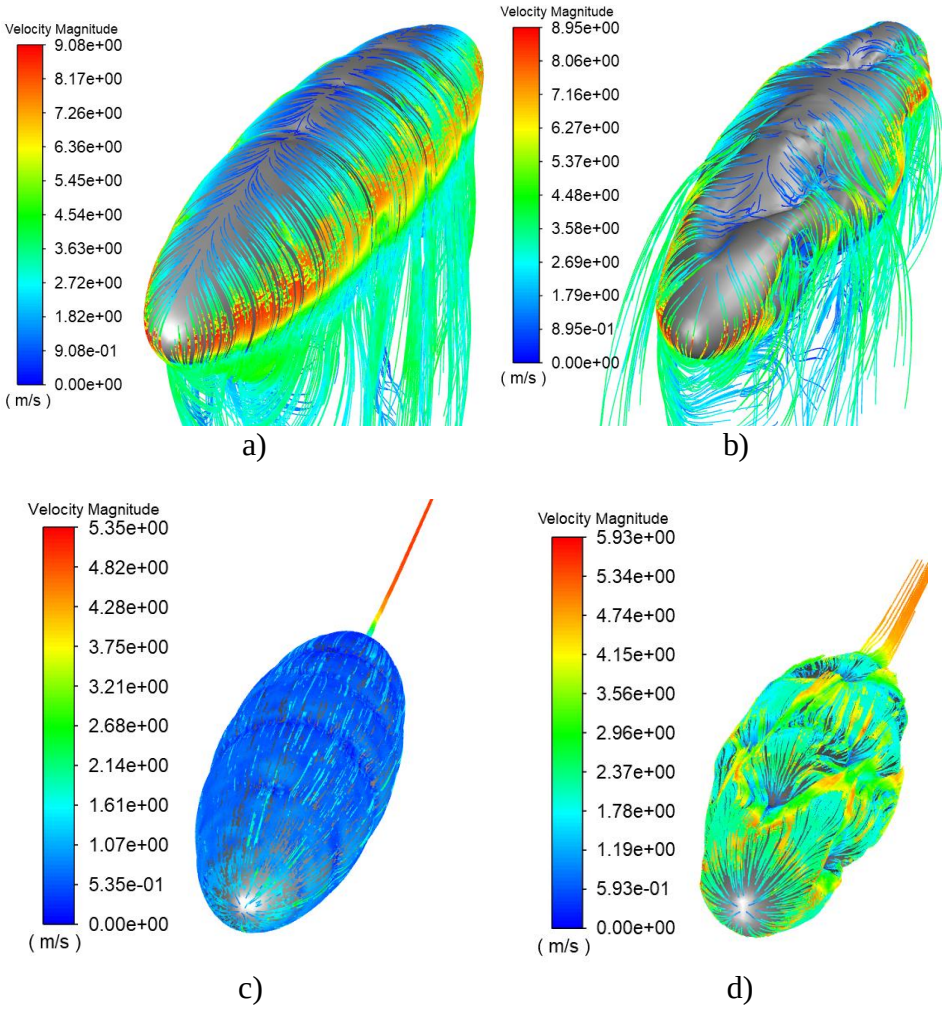

Figure 5. Pathlines of the air flows computed for the vertical and horizontal aerostat velocity of: 5 m/s and altitude a) and c) h_2 , b) and d) h_s.

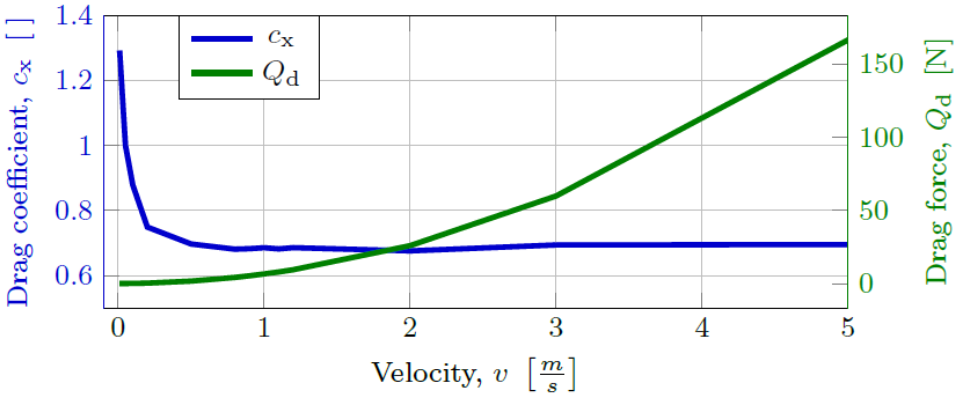

Figure 6. Example of numerically determined dependencies of the drag coefficient c_x and the drag force Q_d for vertical velocities at the altitude h_2

force Q_d and drag coefficient c_x in terms of velocity of the flow (Fig.6). In Fig.7 we have shown change of coefficient c_x for various forms of the aerostat, which depend on the applied method of control. The particular forms correspond to: form 1 - aerostat maximally inflated with helium, form 2 - nominal volume V_0, form 3 - shortening of tendons (3a - in all chambers, 3b - in the middle chamber, 3c - in the outermost chambers). The change of drag coefficient corresponding to lateral flow was further used in analytical model of vertical motion of the aerostat. In turn, the change of drag coefficient corresponding to axial flow was further used in a model of horizontal motion of the aerostat.

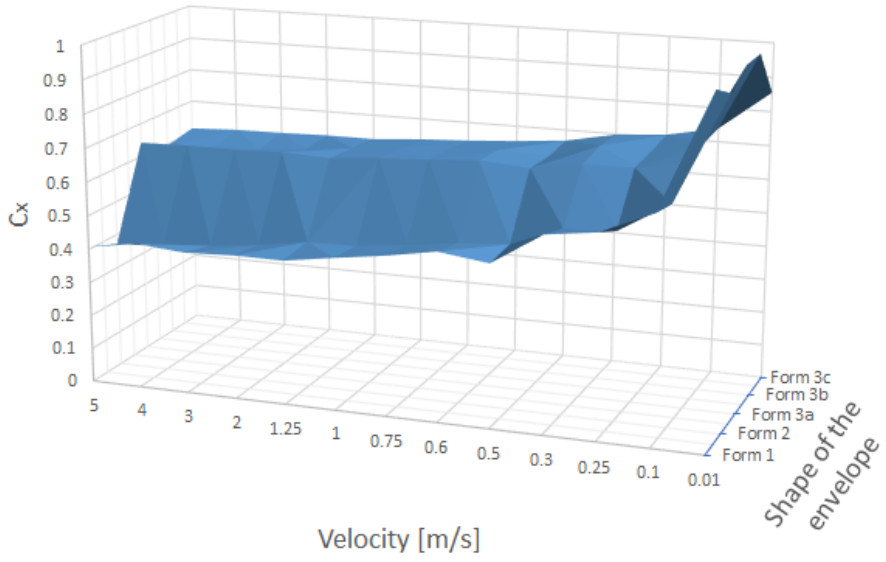

Figure 7. Numerically determined dependence of the coefficient c_x on vertical velocity for different forms of the aerostat

4.2. FSI analysis

The presented study is focused on investigation of the interaction of tensegrity structure and envelope of helium-filled aerostat so the air flow analysis is limited to steady-state conditions. The cases considered in this subsection are focused on the air flow with two speeds applied in the Z-direction (V-mobility). In the first case, the wind velocity increases up to 1.2 m/s (mean velocity during ascend of the aerostat) whereas in the second scenario the air speed reaches 5 m/s (an excessive air flow). In both cases, after time t_0=2.5s the air velocities remain constant. The assumed air density corresponds to the air at ground level, i.e. ρ_a=1.225 kg/m^3.

A computational domain has dimensions: 80 m (Z-direction) by 30 m, (Y-direction) by 14 m (X-direction) and is presented in Fig.8a, whereas the air speed loads are shown in Fig.8b. The velocity boundary condition is applied to the top surface of the cuboid domain. On the bottom surface, the air pressure is expected to be zero and air flows by sidewalls of the computational domain are not permitted. The distances between aerostat semi-axes and computational domain boundary are equal: 10 m (to the top surface along Z-direction), 7 m (along X-direction) and 15 m (Y-direction).

The response of the aerostat is computed utilizing coupled Eulerian-Lagrangian technique with uniform mass scaling applied to the aerostat structure (Lagrangian domain). An air flow (Eulerian domain) interacts with the aerostat membrane by means of defined Eulerian-Lagrangian contact. Due to applied mass scaling, the natural time scale of this dynamic process is perturbated. This, however, can be neglected since only the steady-state deformation of the aerostat, obtained after sufficiently long time of exposure to the gust load, has to be considered.

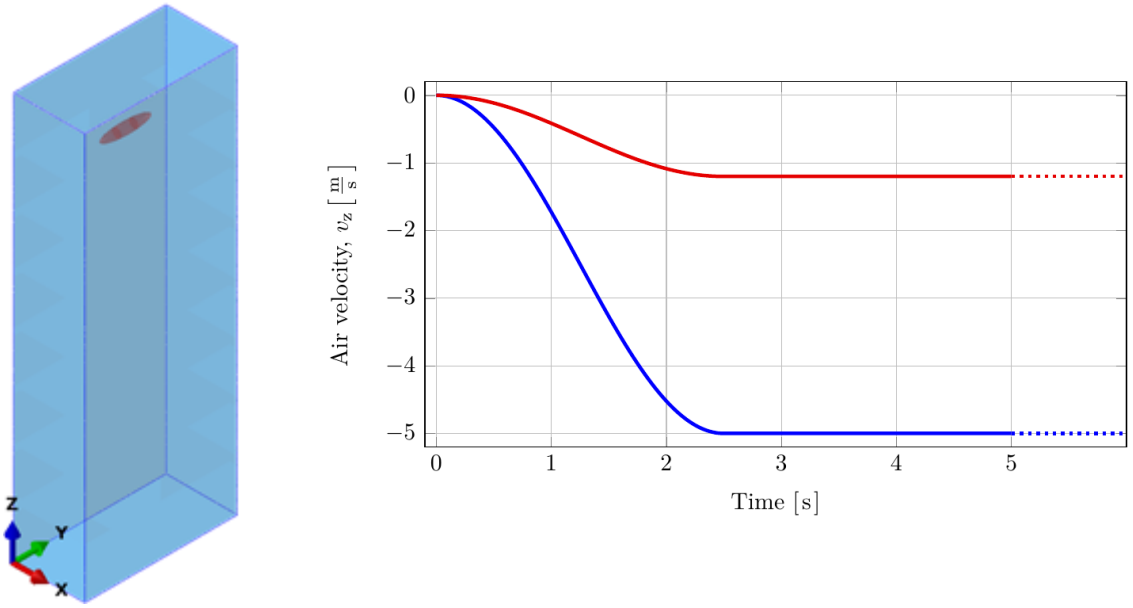

(a) (b)

Figure 8. (a) Computational domain with the initial configuration of the aerostat, (b) velocity functions applied for the air gust loads.

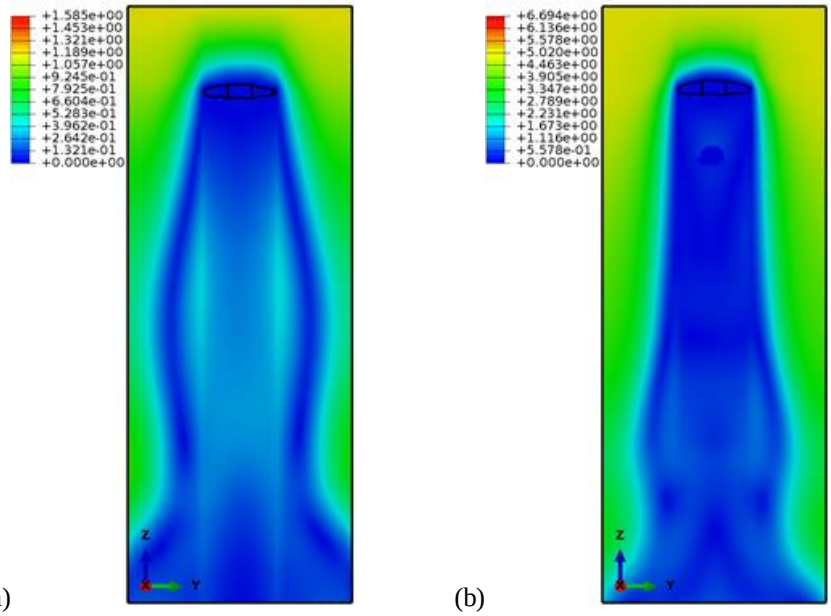

(a) (b)

Figure 9. Velocity contour plot of the air flow subjected to air wind load: (a) 1 m/s, (b) 5m/s.

The aerostat membrane deformation and equivalent von Mises stresses computed for the wind speed 5m/s are shown in Fig.10a. The obtained numerical results show that the mean value of helium pressures reach 20 Pa and 400 Pa in middle chamber and lateral chambers, respectively. The equivalent von Mises stresses locally reach significant values only in stiffening plates (see Fig.10a) and the supporting structure (see Fig.10b). However, they do not exceed tensile strength for carbon fibre which is above 1 GPa. Moreover, the aerostat shape becomes one-side slightly curved. This modified aerostat shape also has influence for the air flow, which is illustrated in Fig.9 for both wind load cases.

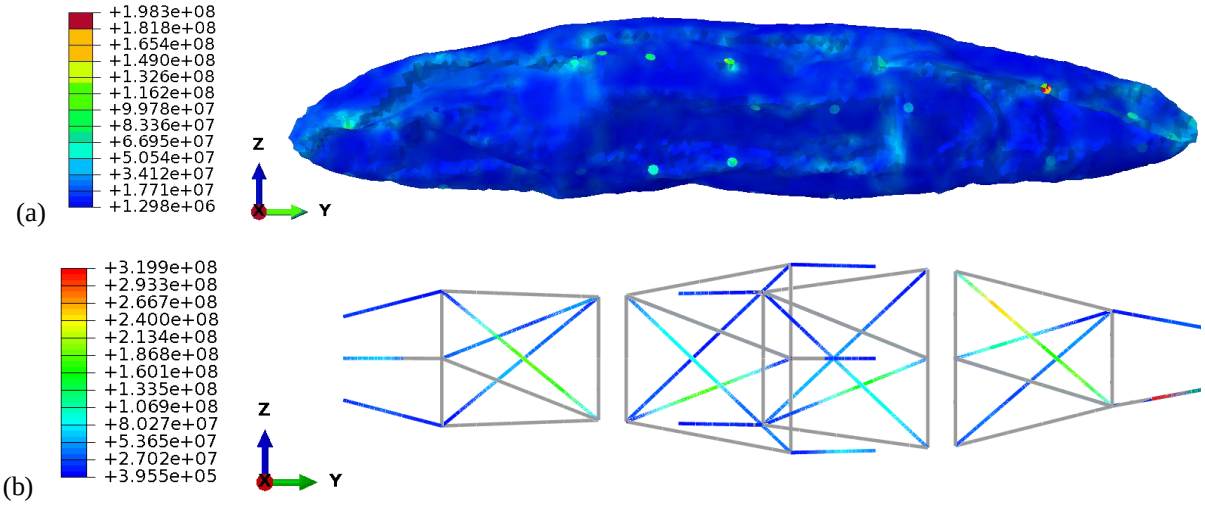

Figure 10. Equivalent von Mises stresses (Pa) in the aerostat membrane (a) and supporting structure (b) caused by the air wind loads with the speed of 5 m/s.

5. CONCLUSIONS

The conducted numerical simulations prove the feasibility of the proposed concept of tensegrity based aerostat. In particular, the strength analysis has shown low values of stresses generated in aerostat envelope and skeletal structure as a result of pressure difference during quasi-static process of aerostat vertical movement. The stresses generated as a result of shortening of the active tendons of tensegrity structure appeared to be significantly larger, but below the strength limit of the applied material. This indicates that control of the aerostat shape and resulting control of its motion can be successfully executed by the proposed methods of tendons shortening. Moreover, the conducted CFD and FSI analyses have shown large values of stresses generated in carbon fiber bars of the tensegrity structure under the wind flow. This indicates that for larger aerostats further optimization of topology and mechanical properties of the applied tensegrity structures is required and have to be developed in the next stage of the conducted research.

ACKNOWLEDGMENTS

The authors acknowledge the support of the National Centre for Research and Development and the National Science Centre, Poland, granted in the framework of the TANGO 4 programme (project TANGO-IV-C/0001/2019-00) and the project DEC-2017/25/B/ST8/01800 of the National Science Centre, Poland.

REFERENCES

[1] Brayan T, Rava G., British airships 1905-1930, Osprey Publishing, New York, 2009.
[2] Ege L. Baloons and Airships. Blandford Press, London, 1974.
[3] Freedman A. Zeppelin Fictions and the British Home Front, Journal of Modern Literature, Vol. 27, No. 3, Writing Life/Writing Fiction, pp. 47-62, Winter, 2004.
[4] Ghanmi A., Sokri A., Airships for military logistics heavy lift, Defence R&D Canada.
[5] Centre for Operational Research and Analysis, DRDC CORA TM 2010-011, 2010.
[6] Future Aerostat and Airship Investment Decisions Drive Oversight and Coordination Needs, Report to the Subcommittee on Emerging Threats and Capabilities, Committee on Armed Services, U.S. Senate, GAO, 2012.
[7] Saleh S., Weiliang HE., New design simulation for a high-altitude dual-balloon system to extend lifetime and improve floating performance, Chinese Journal of Aeronautics, Vol 31, No 5, pp. 1109-1118, 2018.
[8] Araripe d'Oliveira F., Lourenço de Melo F. C., Devezas T. C. High-Altitude Platforms – Present Situation and Technology Trends, J. Aerosp. Technol. Manag., São José dos Campos, Vol.8, No 3, pp.249-262, 2016.
[9] Lee M, Smith S, Androulakakis S (2009) The high altitude lighter-than-air airship efforts at the US Army Space and Missile Defense Command/Army Forces Strategic Command. Proceedings of the 18th AIAA Lighter-Than-Air Systems Technology Conference; Seatle, USA.
[10] K. Eguchi, Y. Yokomaku and M. Mori, "Overview of Stratospheric Platform Airship R&D Program in Japan", in AIAA 14th LTA TCCE, Acron, OH, July 2000.
[11] Airbus, Zephyr S set to break aircraft world endurance record [accessed 30 Jun 2021], https://www.airbus.com/newsroom/press-releases/en/2018/07/Zephyr-S-set-to-break-aircraft-world-endurance-record.html.
[12] Augur RosAeroSystems, High Altitude Airship "Berkut"; [accessed 30 Jun 2021], http://rosaerosystems.com/projects/obj687.
[13] ElectronicsWeekly.Com Airship set to become the ultimate eye in the sky; [accessed 30 Jun 2021], https://www.electronicsweekly.com/news/business/information-technology/airship-set-to-become-the-ultimate-eye-in-the-sky-2011-08
[14] Tales, What's up with Stratobus? [accessed 30 Jun 2021], https://www.thalesgroup.com/en/worldwide/space/news/whats-stratobus
[15] Mizuta E., Akita D., Fuke H., et al, Development of a 2,5 um Plyethylene Film for the Hihgh Altitude Ballon, Trans JSASS Space tech Japan, Vol 7, No 26, 2009.